CONFERENCE PRE-PRINT

RESEARCH AT THE KURCHATOV INSTITUTE IN SUPPORT OF THE CREATION OF A HYBRID FUSION-FISSION SYSTEM

Yu.S. SHPANSKIY^{1,2}
¹National Research Centre "Kurchatov Institute"
Moscow, Russia
²National Research University "MPEI"
Moscow, Russia
Email: Shpanskiy YS@nrcki.ru

M.L. SUBBOTIN
National Research Centre "Kurchatov Institute"
Moscow, Russia

Abstract

Combining nuclear fusion and fission reactions in a single design allows achieving fundamentally new characteristics and parameters of nuclear power systems. Over the past few years, the National Research Centre "Kurchatov Institute" has been working on the feasibility and creation of a pilot hybrid reactor facility (PIHRF) for the integrated commissioning of fusion and nuclear technologies [1-3]. Such a facility could ensure the production of fuel isotopes for both fusion (tritium, if necessary) and nuclear (233 U) reactors. It is assumed that such a facility containing a hybrid blanket, based on a steady-state tokamak with a DT fusion power of more than 30 MW (this corresponds to the generation of $\sim 1\cdot 10^{19}$ neutrons/s) and a fission power of up to 500 MW.

1. INTRODUCTION

The purpose of the work is to implement an R & D program justifying the construction of a hybrid reactor facility (HRF) containing a hybrid blanket based on a stationary tokamak with a DT fusion power of over 30 MW (this corresponds to the generation of $\sim 1~10^{19}$ neutrons/s) and a fission power of up to 500 MW. At this stage, the goal of the work is to carry out systemic studies to develop an experimental prototype (TIN-1) of a pilot scale fusion neutron source on the scale of the T-15MD tokamak to study the process of obtaining uranium-233 from natural thorium-232 by irradiating samples containing thorium-232 with a thermonuclear neutron flux.

Environmentally sound nuclear power (NP) is an important component of the global energy system today. Global electricity and thermal energy consumption is steadily increasing, while the use of fossil fuels is leading to global environmental problems, making NP increasingly important. However, challenges associated with nuclear fuel production, reprocessing, and disposal of radioactive waste from fission reactors impose significant limitations on the development of NP. Fusion technologies based on the fusion of light nuclei of hydrogen isotopes—deuterium and tritium—open new possibilities for optimizing the neutron balance in nuclear power. The integration of fusion technologies for light nuclei and the fission of heavy isotopes of transuranic elements should ensure the long-term and sustainable development of the global energy system. The work carried out at the National Research Centre "Kurchatov Institute" (NRC "KI") on this topic is aimed at the development and construction of a HRF facility.

Until recently, a small-sized, compact thermonuclear neutron source, TIN-C (R \sim 0.5 m, A = 1.6, V_{pl} \leq 2.5 m³), with a fusion power of 3 MW, corresponding to a generation of \sim 10¹⁸ n/s, was being developed for testing materials and components of hybrid systems. However, given the successful launch, start of operation, and initial encouraging results of the T-15MD tokamak [4], a decision was made to develop TIN-1, built using the technologies and solutions adopted during the design and construction of the T-15MD tokamak (Fig. 1), but taking into account its adaptation to the tasks of a fusion neutron source. Thus, at present, the main goal of the ongoing work is R&D to justify the development of an experimental prototype of a thermonuclear neutron source (TIN-1) on the scale of the T-15MD tokamak in support of the PIHRF, the construction of which is the overall goal. At the current stage, the goal is to develop and validate the technology for the production, extraction and purification of 233 U from the working material of the blanket containing the natural isotope 232 Th, as well as to assess the possibility of transferring the developed technologies and achieved results to the PIHRF project.

2. SYSTEM ANALYSIS OF TIN-1

As part of the planned strategy, preliminary assessments of the TIN-1 parameters were conducted. The fusion power level in the TIN-1 was assumed to be 5-10 MW, with the primary contribution to fusion reactions expected to come from beam-plasma reactions. The fast atom injectors were then expected to perform three functions: heating the plasma, generating neutrons, and current drive. The average specific neutron load on the first wall was assumed to be 0.1 MW/m^2 .

The TIN-1 tokamak aims to identify modes that could be useful for developing fusion-fission energy, specifically, using neutrons from the D-T reaction to demonstrate the production of nuclear power plant fuel from 232Th. These modes are related to the fulfilment of a number of criteria:

- achieving long-term plasma burning with a high neutron yield;
- thermonuclear enhancement factor $Q = P_{\text{fus}}/P_{\text{aux}} > 0.3$;
- neutron flux density of the D-T reaction at the first wall $Nn>10^{12}\ neutrons/cm^2/s.$

This paper presents the latest (2024-2025) results of the TIN-1 development. System analysis were conducted to determine and analyse the parameters of the TIN-1 facility with a "warm" copper alloy magnetic system. The baseline parameters were similar to those of the T-15MD: $R_0 = 1.48 \text{ m}$, $B_{t0} = 2 \text{ T}$, $I_P = 2 \text{ MA}$, A = 2.2. During the systemic analysis, the parameters were varied within the range of $R_0 = 1.2$ -1.8 m, $B_{t0} = 1$ -5 T, $I_P = 1$ -5 MA, discharge time = 1-500 s.

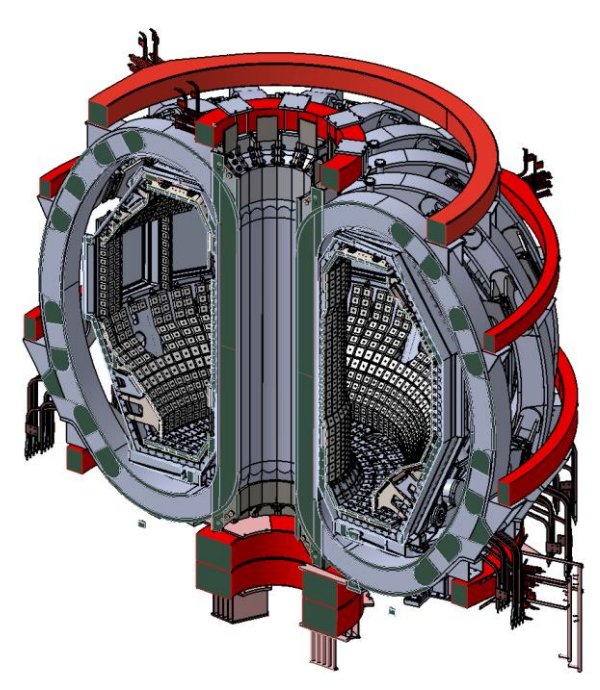


FIG. 1. T-15MD tokamak vertical cross-section view

Plasma heating system at TIN-1 is expected to be based on positive-ion injectors with a maximum particle energy of 140 keV. P_{aux} is expected < 20 MW. This is due to the problems of beam injection into compact facility. During the first parameter iteration, it was assumed that the current density values along the EMS conductor (primarily the toroidal coil (TFC) and the central solenoid (SC), which are "clamped" on the inner edge of the toroid) are 20 MA/m². It is assumed that the CS in the TIN-1 is located outside the toroidal coil. Toroidal coil current value (j_{TF}) for the TIN-1 tokamak was selected. However, for a warm magnetic system, an increase in j_{TF} shortens the discharge duration due to the heating of the conductor during discharge. A reasonable compromise for the j_{TF} value in the TIN-1 project appears to be ~ 10-15 MA/m². The lower value (10 MA/m₂) is closer to the steady-state operation of the facility, while the upper value (15 MA/m²) is closer to a long pulse (tens of seconds). Scenarios for the current density in the TF coil and the CS are presented in Fig. 2.

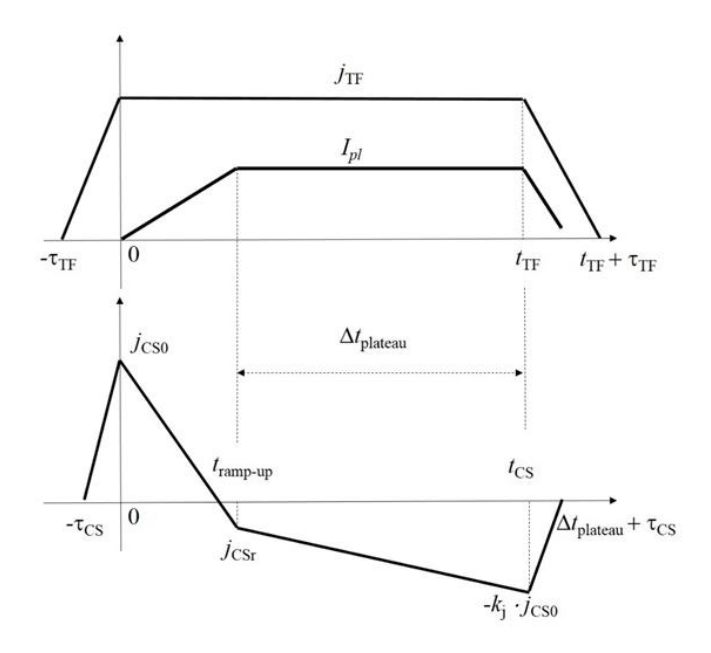


FIG. 2. Scenarios for the current density in the TF coil, at the top, and in the SC at the bottom

Indexes TF – toroidal field, pl – plateau, CS – central solenoid;

 $k_i = 1$ corresponds to complete magnetization reversal, $k_i < 1$ – incomplete.

The current density j_{CSr} when the plasma current reaches the plateau is determined by the flux balance. The plasma current rise time; $t_{ramp-up} = 2$ s, plasma current plateau duration Delta $t_{plateau} = 10$ s.

3. NEUTRAL INJECTION EFFICIENCY ANALYSIS

The efficiency of neutral injection (NI) into the plasma of the TIN-1 tokamak was analysed using the T-15MD geometry. To analyse the efficiency of neutral injection and study the two-component plasma of FNS facilities (of any geometry), it is necessary to use a comprehensive approach that takes into account all beam losses during its formation and transport to the plasma, as well as its "recoil" in the plasma—in the form of fast ion current generation and increased fast ion reactivity. This can be achieved using models that combine a statistical description of the beam with analytical methods for calculating particle trajectories, as is done in the BTR-BTOR model [5]. In the range of 50–150 keV, with increasing beam energy, the total neutron yield increases due to the increased intensity of D-T reactions during beam-plasma interactions. With increasing beam energy, a significant increase in the efficiency of plasma current generation by fast ions is also observed. However, due to the relatively small plasma volume, the beam energy is limited by the thermal load on the tokamak chamber wall, which increases with increasing atomic energy due to decreased plasma capture. The injection scheme for the T-15MD is shown below (Fig. 3). Basic plasma parameters: density: $(3 \div 7) \times 10^{19}$ m⁻³, distribution – cubic parabola. Maximum electron temperature (on axis) $Te = 2 \div 6$ keV, distribution – quadratic parabola (average plasma density $(0.5-1) \times 10^{20}$ m⁻³). Plasma current: $Te = 1 \div 2$ MA. Toroidal magnetic field: $Te = 1 \div 2$ T; elongation $te = 1.6 \div 1.8$; triangularity $te = 0.2 \div 0.5$.

Since 2018, the BTOR (Beam-in-TORoids) software package, registered in 2019, has been used to study the efficiency of a neutral beam in a plasma volume, taking into account the influence of geometric factors, including the toroidal geometry of the magnetic field. The statistics of beam particles entering the plasma and their transformation into fast ions are calculated using the BTR code [5]. The subsequent behaviour of each fast ion is determined by its birth point in cylindrical coordinates, the angle of departure relative to the magnetic field at this point (initial pitch angle), and the deceleration (or thermalization) time. The deceleration time and the full path of fast ions in the plasma are calculated using classical deceleration theory. Although this "system-statistical" approach to describing the birth and behaviour of fast ions in plasma is relatively simple and does not take into account ion drift motions, it is entirely valid for analysing the magnetized plasma regimes with a low collision rate characteristic of FNSs and allows for a clear interpretation of the results. Furthermore, it naturally allows for optimization of injection parameters. It should be noted that using classical tokamak scaling is not always feasible for the proposed FNS scenarios. Comparison of the BTOR results with similar calculations using the ASTRA code suggests good agreement for classical tokamaks (for R/a>3), in which toroidal effects during the slowing down of fast ions are negligible. The beam injection model for the TIN-1 plasma is shown in Fig. 4.

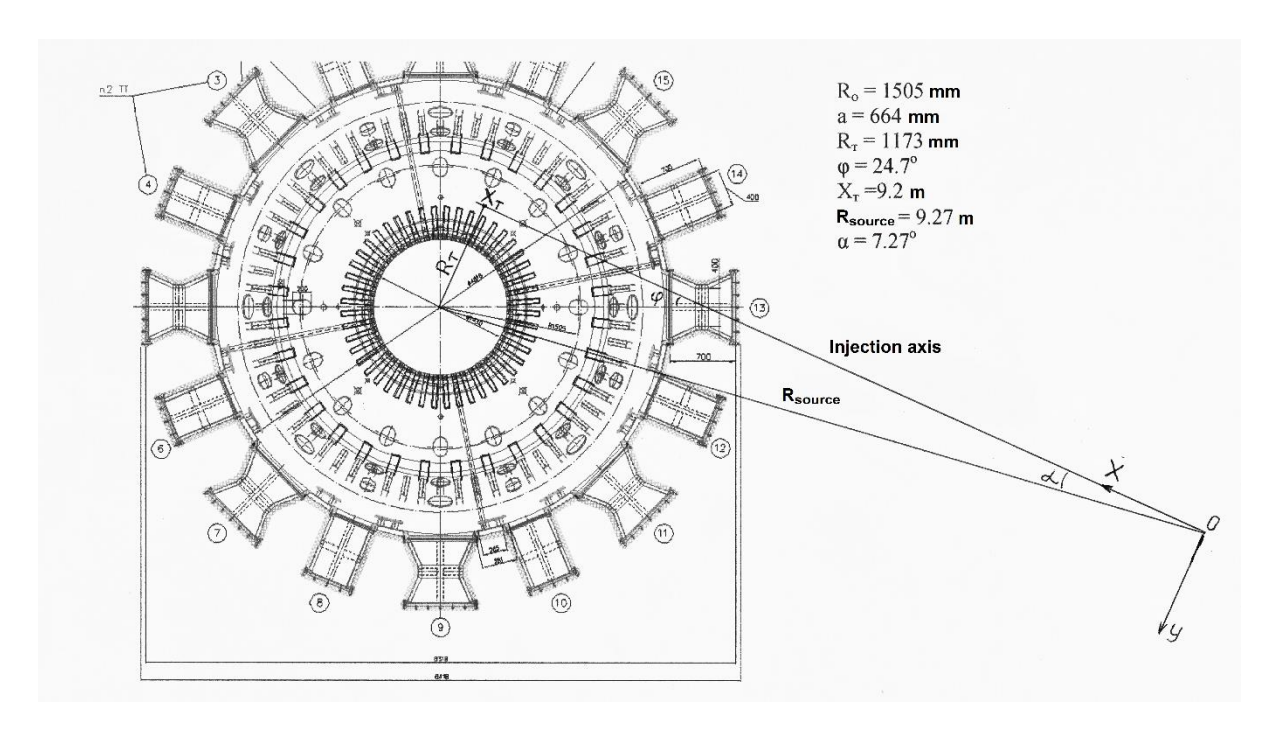


FIG. 3. Injection scheme

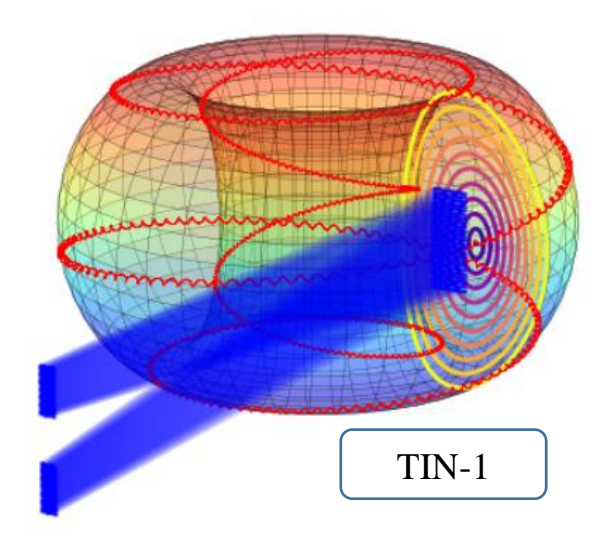


FIG. 4. Beam and plasma model in the BTOR code. The trajectory of the magnetized ion is shown in red.

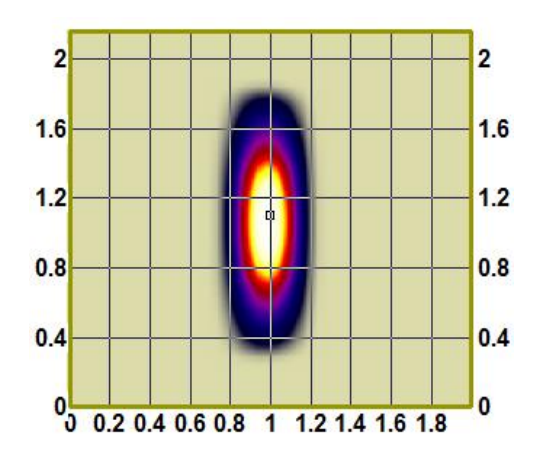
Examples of 2-dimensional heat load maps from neutral injection power that passed through the plasma (i.e., was not trapped in the plasma) are shown in Figures 5 and 6. In designations Energy/H+ ion current/neutralization:

- 1. Option 1 (50 keV /90A /53%, power after neutralizer $P_N = 2,37$ MW, injection power $P_{inj} = 2,25$ MW);
- 2. Option 2 (50 keV /90A /53%, $P_N = 2.37$ MW, $P_{inj} = 2.25$ MW) (without molecular ions yet).

Increasing the injection energy from 60 to 120 keV increases the neutron yield by approximately three times. At an injection power of 8 MW, the beam neutron yield will be 1.3×10^{17} (60 keV) and 4.2×10^{17} (120 keV) at a plasma electron temperature of 5 keV. Increasing the plasma temperature to 10 keV increases the neutron yield by 15-20%, but the intensity of neutron generation in reactions between thermal ions increases by an order of magnitude, making high-temperature plasma modes the most attractive for FNS facilities.

Table 1 presents estimates of the maximum neutron yield from 1 MW of injected power in the form of deuterium in the energy range 60-140 keV. The maximum yield is achieved by releasing fast ions in the central, hottest region of the plasma.

[Left hand page running head is author's name in Times New Roman 8 point bold capitals, centred. For more than two authors, write **AUTHOR et al.**]



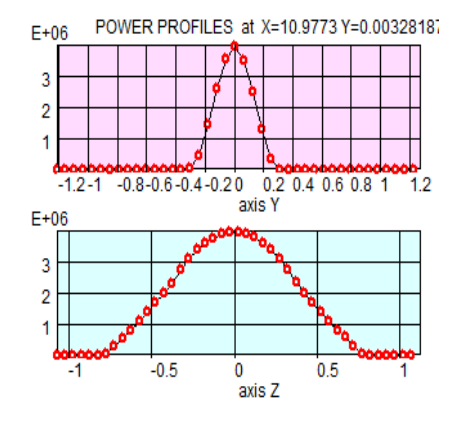
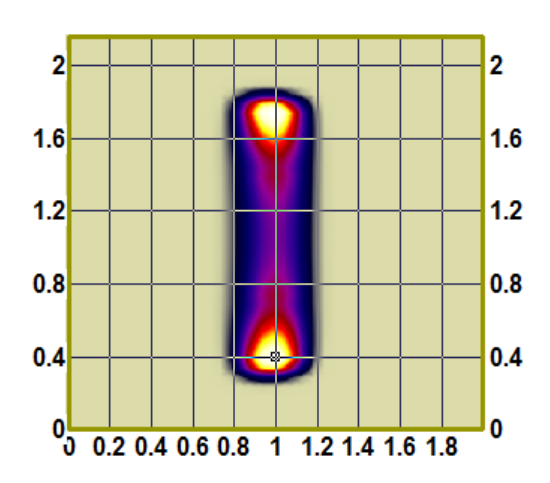


FIG. 5. Thermal power map on the first wall of the TIN-1 tokamak chamber (Option 1).



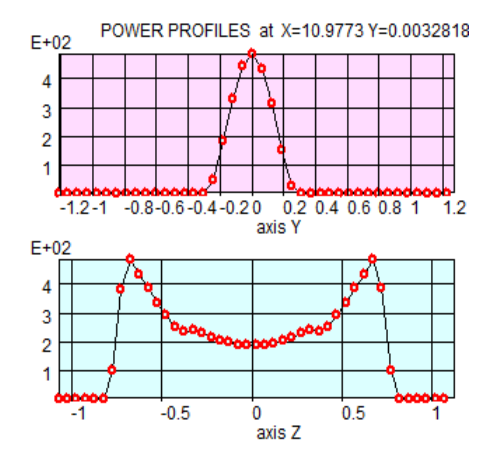


FIG. 6. Thermal power map on the first wall of the TIN-1 tokamak chamber (Option 2).

TABLE 1. Maximum neutron yield from a 1 MW deuterium beam injected into the TIN-1 tokamak plasma

Energy of the main component of the deuterium beam, $E_{\rm full}$ keV	Current of the main component atoms in 1 MW of injected power,	Plasma electron temperature on the axis, Te, keV	Plasma electron density on the axis, n _e , m ⁻³	Neutron yield from 1 MW injection $(E_{full} + E_{1/2} + E_{1/3}), Y_{NB},$ n / s
60	10	5	1×10 ²⁰	1,6×10 ¹⁶
80	7,5	5	1×10 ²⁰	3,1×10 ¹⁶
100	6	5	1×10 ²⁰	4,4×10 ¹⁶
120	5	5	1×10^{20}	5,2×10 ¹⁶
140	4,3	5	1×10 ²⁰	5,7×10 ¹⁶
60	10	10	1×10 ²⁰	1,9×10 ¹⁶
80	7,5	10	1×10^{20}	3,5×10 ¹⁶
100	6	10	1×10 ²⁰	5,0×10 ¹⁶
120	5	10	1×10 ²⁰	6,0×10 ¹⁶
140	4,3	10	1×10 ²⁰	6,4×10 ¹⁶

4. NUMERICAL ANALYSIS (BENCHMARK) OF CYCLIC LOADING ON A DIVERTOR

A numerical benchmark of the test model of the divertor plate loaded by a cyclic heat flux of 25 MW/m^2 was carried out. Full-scale tests were carried out in the research department of JSC "NIIEFA" [6]. Test samples of multilayer plasma-facing elements (first wall and divertor targets) operating at a thermal load up to 25 MW/m^2 are shown in Fig. 8.

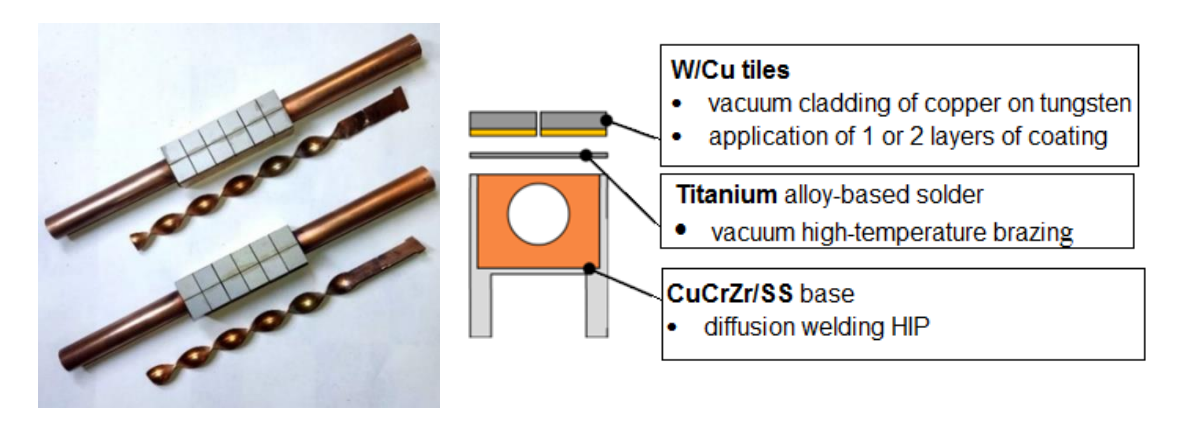


FIG. 8. Prototypes of multilayer plasma-facing elements with swirled tapes

Cooling Parameters:

water coolant pressure 3.9 MPa; inlet coolant temperature 115 °C; coolant velocity 10 m/s.

Thermal cycling at a maximum thermal load of 25 MW/m² for at least 300 cycles without significant damage. A total of 1000 consecutive cycles were performed - 15 seconds pulse and 15 seconds' pause. The results of thermal-hydraulic (Fig. 9), thermal and strength analysis are presented in Fig. 10.

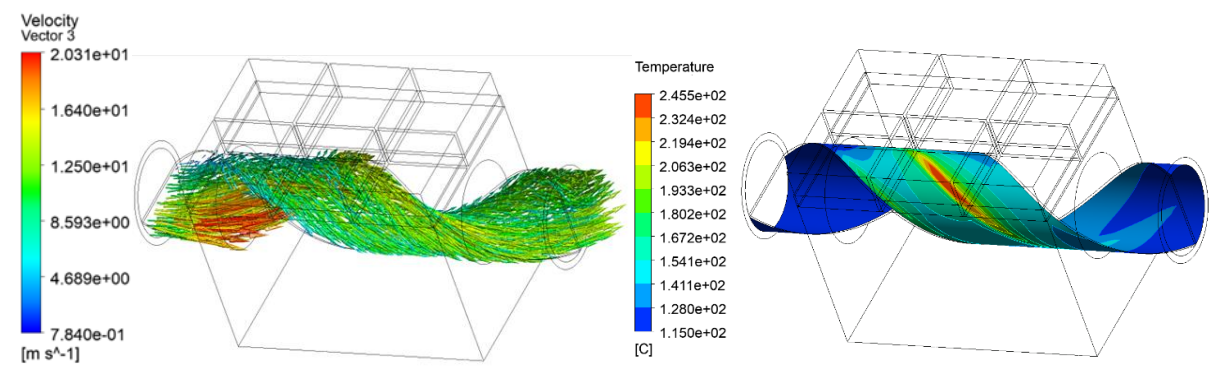


FIG. 9. Velocity vectors of coolant (water) in 1/2 part separated by a swirler coolant channel (a) temperature field in the water at the border with the vortex (b)

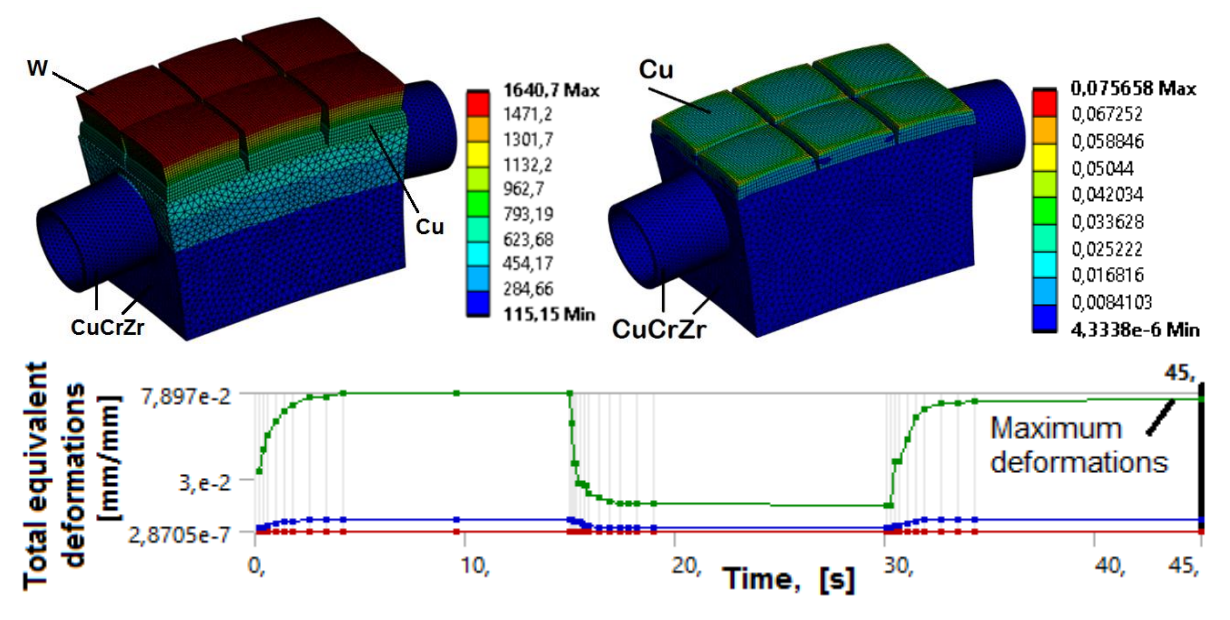


FIG. 10. Temperature fields (°C) in the structure in 45 s (a), total equivalent deformations in the copper layer and heat transfer unit (CuCrZr) in 45 s (b), graph of total equivalent deformations from loading time, (c)

The results of numerical thermal and thermal-hydraulic analysis demonstrate full compliance with the results of the full-scale experiment. Subsequent strength and cyclic analysis based on models of deformation approaches and fatigue experimental data of materials determined the number of cycles before the onset of local fractures or cracking. **For Cu, this number was 54 cycles.** Provided the copper substrate is intact and does not delaminate from adjacent elements, this number for CuCrZr is 10110 cycles, and for W, 291000 cycles.

5. MATERIALS SCIENCE. GAS BUBBLE EVOLUTION IN STEEL 316 UNDER ANNEALING: THEORY AND EXPERIMENT

Helium atoms result from threshold transmutation reactions (n, α) in structural materials of nuclear fission and fusion reactors. Helium is produced by neutrons mainly on Ni and Cu [7]. An increased helium and hydrogen production on Fe in fusion reactors is also observed [8]. Helium and hydrogen facilitate the generation and growth of cavities in metals and alloys irradiated in the homologous temperature range from $0.3T_m$ to $0.5T_m$. At high temperatures, $>0.5T_m$, a number of thermal vacancies in metal is significant and, together with gas atom transport, affect the bubble accumulation due to the edge dislocation climb in metals and grain boundaries influencing. Asymptotic approach taken from the Lifshitz-Slezov (LS) theory is used for the description of the evolution of two-component gas-vacancy clusters (bubbles) in metals during annealing [9, 10]. Time and temperature dependences obtained for the average radius R and the total bubble density N are formulated on a basis of the approach we proposed in [9]. Temperature dependences given in [10] were compared with the results of an experimental study [11]. It was shown that the most probable bubble growth mechanism during annealing of metals implanted with helium is the Ostwald ripening (OR) mechanism. Of particular interest is the analysis of experimental data on 316L austenitic stainless steel using as a structural material in light water and fast breeder reactors. It is also known that 316L(N) steel was chosen for being a primary structural material for the ITER nuclear fusion reactor project.

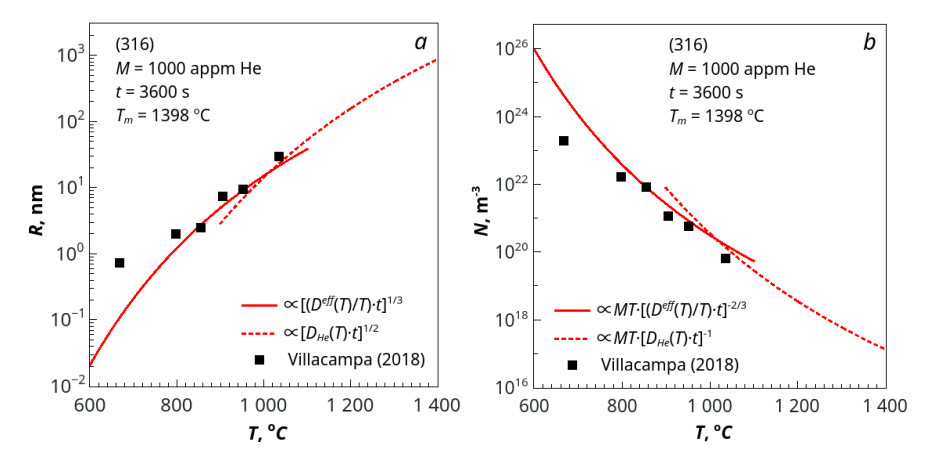


FIG. 7. Comparison of the experimental measurements in steel 316 (black squares indicate data from [5]) with the temperature dependences for R (a) and for N (b) according to the OR model.

Material parameters for austenitic stainless steel 316 shown in Table 2 were used in theoretical evaluation of growing bubbles in the steel during annealing.

TABLE 2. Material parameters for austenitic stainless steel

Parameter	Value	Reference
Amount of implanted helium atoms M , appm	1000	[10]
Lattice constant a, Å	3.58	[12]
Atomic volume Ω , m ³	11.47e-30	[13]
Surface energy γ, J/m ²	2.00	[14]
Helium dissociation energy ψ, eV	2.4	[15]

The experimental data of [5], as shown in Figure 1, are generally in good agreement with theoretical dependences $R \propto [(D^{eff}(T)/T) \cdot t]^{1/3}$ and $N \propto MT \cdot [(D^{eff}(T)/T) \cdot t]^{-2/3}$ in the temperature range < 1010 °C. However, at the temperature 650 °C, when R < 1 nm, a noticeable discrepancy between the theory and experiment is observed. The reason for this discrepancy is probably the same as in the case of Ni, i.e. because of TEM limitations. The

[Right hand page running head is the paper number in Times New Roman 8 point bold capitals, centred]

authors of the work [5] also noticed that a significant number of bubbles were below actual resolution of TEM (< 2 nm) at the temperature 650 °C. The experimental data obtained in austenitic steel allow a comparison with theoretical estimates of $R \propto [D_{He}(T) \cdot t]^{1/2}$ and $N \propto MT \cdot [D_{He}(T) \cdot t]^{-1}$ which characterize the evolution of large bubbles. In Figure 1 it is evident that the experimental data taken at the temperature 1050 °C are in consistent with the theory. Thus, the plotted theoretical dependences reproduce the experimental observations well both for small and larger bubbles. Therefore, bubble growth in 316 austenitic steel is most likely due to the OR mechanism. The comparative analysis of theoretical and experimental data has shown that gas bubble evolution differs at early and later stages of coalescence. Different-sized small and larger bubbles grow at different rates. Nevertheless, asymptotic solutions are identical for monoatomic and polyatomic gases. The solution obtained to the problem of decomposition of two-component gas-vacancy solution appeared to be similar to that given by the LSW theory.

6. CONCLUSION

R & D activities are being performed in NRC "Kurchatov Institute" of an experimental prototype of a fusion neutron source (TIN-1) on the scale of the T-15MD tokamak in support of the pilot industrial hybrid reactor facility. System analyses of designed TIN-1 facility based on "warm" MS were caried out. In 2025-2026, it is planned to analyze the designed TIN-1 facility with a cryoresistive magnetic system.

7. AUTHORS AFFILATION

Main contributors:

^{1,2}Yu.S. SHPANSKIY, ¹M.L. SUBBOTIN, ^{1,2}V.P. BUDAEV, ³A.B. MINEEV, ¹E.D. DLOUGACH, ¹A.V. KLISCHENKO, ¹A.M. OVCHARENKO

ACKNOWLEDGEMENTS

The work was carried out in accordance with the Russian Federation state assignment of the National Research Centre "Kurchatov Institute».

REFERENCES

- [1] B.V. KUTEEV, E.A. AZIZOV, P.N. ALEXEEV, et al. // Development of DEMO-FNS tokamak for fusion and hybrid technologies. Nucl. Fusion 55 (2015) 073035 (8pp) p.1-8.
- [2] B.V. KUTEEV, Yu.S. SHPANSKIY et al. // Status of DEMO-FNS development / Nucl. Fusion, 57 (2017) aa6dcb.
- [3] Yu.S. SHPANSKIY and DEMO-FNS Team // Progress in the design of the DEMO-FNS hybrid facility / Nucl. Fusion, 59 (2019) ab14a8.
- [4] P.P. KHVOSTENKO, I.O. ANASHKIN, E.N. BONDARCHUK et al. Experimental Thermonuclear Installation Tokamak T-15MD. Physics of Atomic Nuclei, 83 (2020) 1037.
- [5] E. DLOUGACH, M. KICHIK. Beam Transmission (BTR) Software for Efficient Neutral Beam Injector Design and Tokamak Operation. Software 2023, 2, 476-503 https://doi.org/10.3390/software2040022.
- [6] P.Yu. PISKAREV Report at the technical meeting, NRC "KI", Moscow, February 19-20, 2024.
- [7] V.I. KHRIPUNOV. VANT. Seriya: Termoyadernyy sintez, 45, 2, 5 (2022). (in Russian)
- [8] A.I. BLOKHIN, N.A. DEMIN, V.M. TCHERNOV. VANT. Seriya: Materialovedenie i novye materialy 70, 2006, 108 (2012) (in Russian).
- [9] A.M. OVCHARENKO, I.I. CHERNOV. J. Nucl. Mater. 528, 151824 (2020).
- [10] A.M. OVCHARENKO, Phys. Sol. State. 67, 3, 408 (2025)
- [11] I. VILLACAMPA, J.C. Chen, P. Spätig, H.P. Seifert, F. Duval. J. Nucl. Mater. 500, 389 (2018).
- [12] H. SHINNO, H. SHIRAISHI, R. WATANABE, et. al. J. Nucl. Mater. 97, 291 (1981).
- [13] M.R. HAYNS, J. GALLAGHER, R. BULLOUGH. J. Nucl. Mater. 78, 236 (1978).
- [14] W.R. TYSON. Can. Metall. Q. 14, 4, 307 (1975).
- [15] V. PHILIPPS, K. SONNENBERG, J.M. WILLIAMS. J. Nucl. Mater. 107, 271 (1982).

¹National Research Centre "Kurchatov Institute", Moscow, Russian Federation

²National Research University "MPEI", Moscow, Russian Federation

³Efremov Institute, Sankt-Petersburg, Russian Federation